

# Overcoming Weak Visual-Textual Alignment for Video Moment Retrieval

Minjoon Jung<sup>1</sup> Youwon Jang<sup>2</sup> Seongho Choi<sup>2</sup> Joochan Kim<sup>2</sup>  
Jin-Hwa Kim<sup>3,4,\*</sup> Byoung-Tak Zhang<sup>1,2,3,\*</sup>

<sup>1</sup>IPAI & <sup>2</sup>CSE & <sup>3</sup>AIIS, Seoul National University

<sup>4</sup>NAVER AI Lab

{mjjung, ywjang, shchoi, jckim, btzhang}@bi.snu.ac.kr

jinhwa.kim@navercorp.com

## Abstract

Video moment retrieval (VMR) aims to identify the specific moment in an untrimmed video for a given natural language query. However, this task is prone to suffer the weak visual-textual alignment problem from query ambiguity, potentially limiting further performance gains and generalization capability. Due to the complex multimodal interactions in videos, a query may not fully cover the relevant details of the corresponding moment, and the moment may contain misaligned and irrelevant frames. To tackle this problem, we propose a straightforward yet effective model, called **Background-aware Moment DETection TRansformer** (BM-DETR). Given a target query and its moment, BM-DETR also takes negative queries corresponding to different moments. Specifically, our model learns to predict the target moment from the joint probability of the given query and the complement of negative queries for each candidate frame. In this way, it leverages the surrounding background to consider relative importance, improving moment sensitivity. Extensive experiments on Charades-STA and QVHighlights demonstrate the effectiveness of our model. Moreover, we show that BM-DETR can perform robustly in three challenging VMR scenarios, such as several out-of-distribution test cases, demonstrating superior generalization ability.<sup>2</sup>

## 1 Introduction

Video moment retrieval (VMR) [1] is a challenging task that aims to retrieve the target moment within an untrimmed video corresponding to a natural language query. A successful VMR model requires a strong understanding of videos, language queries, and correlation between inputs to predict relevant moments precisely. In contrast to traditional action localization tasks [2, 3] that predict a fixed set of actions like “throwing” or “jumping,” VMR is more difficult and offers considerable potential for applications such as video retrieval [4] and video captioning [5].

Although previous VMR approaches have yielded promising results, we found that the weak visual-textual alignment caused by the ambiguity of natural language query limits their potential for further performance gains and generalization ability. The complex multimodal interactions in videos can make it difficult for a query to capture all the semantic meanings in a video moment to specify the relevant moment. For example, other events are occurring within the moment that is not expressed in the query, or the boundary annotations may contain irrelevant and noisy frames to the query. Such issues are fundamental challenges since VMR is sensitive to temporal accuracy requiring a

\* Corresponding authors.

<sup>2</sup>Our code is available at: <https://github.com/minjoong507/BM-DETR>

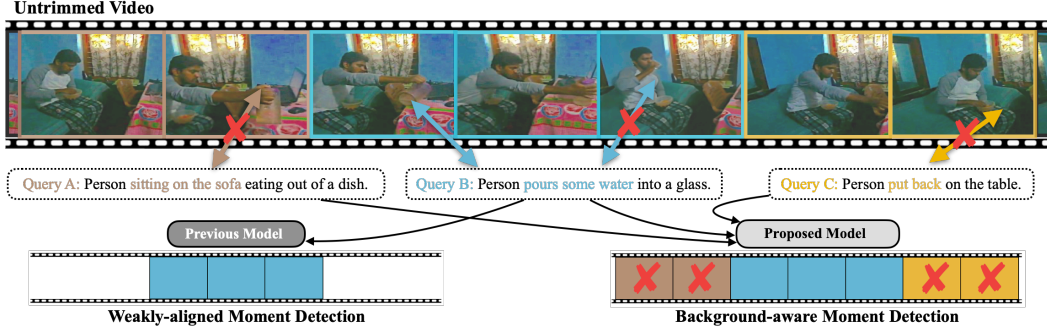


Figure 1: **Top:** We give an example of weak visual-textual alignment in the video. For example, Query B does not explain an event for “drink water” but occurs in Ground-truth B. **Bottom:** We compare the current (left) and proposed (right) VMR approach.

fine-grained visual-textual alignment. While gathering high-quality video-query pairs is a potential solution; however, it may not be practical due to its cost and inefficiency.

The main goal of this work is to devise a method that can effectively learn the representation of both visual and textual inputs, enabling it to achieve better alignment between them and predict the target moment precisely based on multimodal interactions. To this end, we propose a **Background-aware Moment DEtection TRansformer**, called BM-DETR. Here are our main ideas:

As shown in Figure 1, our key observation is that previous approaches only expect a single query as an input query and predict the target moment. However, solely relying on a single query may cause semantic meanings within the video to be overlooked due to weak alignment problems. To solve this problem, several works utilize contrastive learning by maximizing the mutual information between video and query representations (video-query pairs); however, we show that relative relationships between positive and negative queries for the same video are crucial in predicting target moments.

We suggest that utilizing contexts outside of the target moments (*i.e.*, negative queries) along with the target query can enhance overall alignment in videos. Specifically, our model calculates the joint probability of a target query and the complement of negative queries for every potential frame, resulting in frame attention scores. We use these scores to update the multimodal features and then predict the target moment based on updated features. This allows our model to learn how to best identify and focus on the relevant visual features of the target moment, improving *moment sensitivity*, or *true positive rate*. In addition, we leverage a temporal shifting method as an auxiliary objective and learnable spans that helps the model be more robust to temporal content changes and improve further performance. We demonstrate the effectiveness of our model by showing superior performance on Charades-STA [1] and QVHighlights [6] datasets. In addition, we verify the robustness of BM-DETR by conducting comprehensive experiments on three challenging datasets: Charades-CD [7], Charades-CG [8], and Charades-STA Unseen [9], containing out-of-distribution test cases that are representative of real-world scenarios.

To sum up, the contributions of our paper can be summarized as follows:

- In this paper, we argue the weak visual-textual alignment problem from query ambiguity, which is crucial in video moment retrieval tasks.
- We propose BM-DETR that mitigates weak alignment problems by considering background contexts in videos in the model’s prediction process.
- Extensive experiment results on diverse datasets, including challenging VMR scenarios, clearly demonstrate the effectiveness of our proposed methods.

## 2 Related work

**Video moment retrieval.** Video moment retrieval (VMR) aims to retrieve the target moment in a video based on a natural language sentence. Existing approaches are mainly classified into proposal-based methods and proposal-free methods. The proposal-based methods [1, 10–15] sample candidate moments from the video via sliding windows or proposal network and select the most similar moment to the given query. In contrast, proposal-free methods [16–23] regress target moments

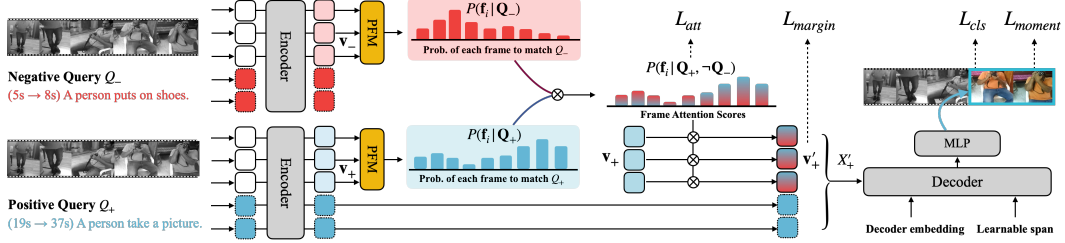


Figure 2: An overview of the proposed BM-DETR framework.

from video and language features without generating candidate moments. These approaches calculate the probabilities of each frame being the start and end points to predict the moments. Recently, several studies [6, 24, 25] have utilized the DETR’s [26] object detection capabilities for localization tasks. Our proposed BM-DETR also follows DETR’s detection paradigm.

**Visual-textual alignment problem in video domains.** Labeling videos is expensive and cumbersome, making it difficult to build high-quality and scalable video datasets. As a result, several studies [27–29] have highlighted the alignment problem between frames and captions in video datasets as a crucial bottleneck of video understanding. In localization tasks, Nan et al. [23] proposed the causality-based model with contrastive learning to diminish spurious correlations between videos and queries and achieve better alignment. Ding et al. [30] proposed a support set concept for VMR using the contrastive objective with generative captioning to consider shared concepts between video-query pairs in the batch. We developed BM-DETR to address alignment problems and show the importance of relation modeling for video-query pairs within the same video. The most similar work to ours is TSP [31], which proposes the pretraining paradigm for localization tasks to improve temporal sensitivity by foreground/background region classification, but it only works with pre-defined action classes.

### 3 Method

#### 3.1 Video moment retrieval task

Given an untrimmed video  $V$  and language query  $Q$ , we represent the video as  $V = \{f_i\}_{i=1}^{L_v}$  where  $f_i$  denotes the  $i$ -th frame. Likewise, the language query is denoted as  $Q = \{w_i\}_{i=1}^{L_w}$  where  $w_i$  denotes the  $i$ -th word.  $L_v$  and  $L_w$  indicate the overall count of frames and words, respectively. We aim to localize the target moment  $m = (t_s, t_e)$  in  $V$  from  $Q$ , where  $t_s$  and  $t_e$  represent the start and end times of the target moment, respectively.

#### 3.2 Background-aware moment detection

Our goal is to address the weak alignment problem and predict target moments precisely. As mentioned earlier, a single query may not be sufficient to disambiguate the corresponding moment due to the weak alignment in videos. That said, predicting the target moment in  $V$  based solely on information from  $Q$  is less informative and ineffective, where the term “information” refers to the knowledge or cues used for accurate predictions of the target moment in  $V$ . Hence, we propose an alternative to resolve this problem inspired by *importance sampling* [32]. Similar to the contrastive learning [33], a specific query  $Q_+$  is designated as the target (positive), while we randomly sampled a negative query  $Q_-$  for each training step. Our main idea is based on two guiding principles, which are as follows:

**Principle 1.** *Negative samples for disambiguation are the remaining queries matched to a moment in the same video  $V$ .*

**Principle 2.** *To avoid spurious correlation, the moments corresponding to  $Q_+$  and  $Q_-$  should be at different temporal locations.*

Let  $P(f_i | Q_+)$  and  $P(f_i | Q_-)$  to be the likelihood of  $i$ -th frame to match the positive and negative query, respectively. We assume these likelihoods are independent since their corresponding moments

are at different temporal locations. Our model predicts the target moment by the joint probability for each frame, and the probability can be represented as:

$$P(f_i | Q_+, \neg Q_-) := P(f_i | Q_+) \cdot (1 - P(f_i | Q_-)).$$

Considering  $P(f_i | Q_-)$ , our model can focus on relatively more important meanings included in the positive query. As a result, it utilizes negative queries to be more informative for the model’s prediction, further improving *moment sensitivity*.

We can learn multimodal relations in videos by applying contrastive loss [33], but this may not be effective when each video is not sufficiently annotated. For example, there are up to only seven queries for videos in Charades-STA [1]. In addition, we will discuss the effect of sampling negative samples from other videos in Section 5.2.

### 3.3 Architecture

We give an overall architecture of the BM-DETR in Figure 2. First, our encoder takes the  $V$ ,  $Q_+$ , and  $Q_-$  as the inputs. Then we obtain frame attention scores from encoder outputs and update them for background-aware moment detection. After our decoder predicts moments from given inputs, we calculate the losses from predictions and ground-truth moments, as in DETR [26]. In addition, we leverage a temporal shifting method to encourage the model’s time-equivariant predictions. The details of the model components are described in the following sections.

#### 3.3.1 Encoder

Our encoder aims to catch the multimodal interaction between video  $V$  and query  $Q$ . Initially, the pre-trained model (e.g., CLIP [34]) is employed to convert each input into multi-dimensional features and normalize them. We utilize two projection layers to convert input features into the same hidden dimension  $d$ . Each projection layer consists of several MLPs. Then, we obtain video representations as  $\mathbf{V} \in \mathbb{R}^{L_v \times d}$  and query representation as  $\mathbf{Q} \in \mathbb{R}^{L_w \times d}$ . Note that there are two query representations  $\mathbf{Q}_+$  and  $\mathbf{Q}_-$  for positive and negative queries, respectively. We direct them to the multimodal encoder  $E(\cdot)$ , a stack of transformer encoder layers denoted as:

$$E(\mathbf{V}, \mathbf{Q}) = E(PE(\mathbf{V}) \parallel \mathbf{Q}),$$

where  $PE$  means the positional encoding function [35],  $\parallel$  indicates the concatenation on the feature dimension. We denote the length of concatenated features as  $L = L_v + L_w$ . Finally, we obtain multimodal features  $X_+$  and  $X_-$  represented as:

$$X_+ = E(\mathbf{V}, \mathbf{Q}_+), \quad X_- = E(\mathbf{V}, \mathbf{Q}_-),$$

where  $X_+ \in \mathbb{R}^{L \times d}$  and  $X_- \in \mathbb{R}^{L \times d}$ .

#### 3.3.2 Implementing the background-aware moment detection

Let us redefine the frame parts of the multimodal features  $X_+$  and  $X_-$  are  $\mathbf{v}_+ = \{\mathbf{f}_i^+\}_i^{L_v}$  and  $\mathbf{v}_- = \{\mathbf{f}_i^-\}_i^{L_v}$ , respectively. We compute the likelihood of each frame to match the positive and negative queries, denoted as  $P(\mathbf{f}_i | \mathbf{Q}_+)$  and  $P(\mathbf{f}_i | \mathbf{Q}_-)$ , respectively. These probabilities can be obtained through a Probabilistic Frame-Query Matcher (PFM) defined as:

$$P(\mathbf{f}_i | \mathbf{Q}_+) = \text{PFM}(\mathbf{f}_i^+), \quad P(\mathbf{f}_i | \mathbf{Q}_-) = \text{PFM}(\mathbf{f}_i^-).$$

PFM consists of two linear layers followed by tanh and sigmoid ( $\sigma$ ) functions defined as:

$$\text{PFM}(\mathbf{f}_i) = \sigma(\tanh(\mathbf{f}_i \mathbf{W}_1) \mathbf{W}_2),$$

where  $\mathbf{W}_1 \in \mathbb{R}^{d \times \frac{d}{2}}$  and  $\mathbf{W}_2 \in \mathbb{R}^{\frac{d}{2} \times 1}$  are learnable embedding matrices. As mentioned in Section 3.2, the joint probability of  $i$ -th frame  $\mathbf{p}_i$  can be calculated as:

$$P(\mathbf{f}_i | \mathbf{Q}_+, \neg \mathbf{Q}_-) = P(\mathbf{f}_i | \mathbf{Q}_+) \cdot (1 - P(\mathbf{f}_i | \mathbf{Q}_-)).$$

After that, the softmax function is applied to obtain the frame attention scores  $\mathbf{o}$ :

$$\mathbf{o} = \text{Softmax}(\mathbf{p}_1, \mathbf{p}_2, \dots, \mathbf{p}_{L_v}).$$

Finally, we leverage  $\mathbf{o}$  to update the positive frame features  $\mathbf{v}_+$  in  $X_+$  to  $\mathbf{v}'_+$ . This can be formulated as follows:

$$\mathbf{v}'_+ = \mathbf{o} \otimes \mathbf{v}_+,$$

where  $\otimes$  is an element-wise product. If there is no negative query in the video, we only use positive visual features  $\mathbf{v}_+$  to obtain frame attention scores  $\mathbf{o}$ . We denote the updated multimodal features as  $X'_+$  and send it to the decoder to predict the target moment.

### 3.3.3 Decoder

To encourage the model to accommodate flexible moments in a video, we introduce learnable spans suitable for our task, which borrowed from DAB-DETR [36]. We denote learnable spans as  $S = \{S_m\}_{m=1}^M$ , and each learnable span is represented as  $S_m = (c_m, w_m)$ , where  $c_m$  and  $w_m$  refer to the center and width of the corresponding span. Given a span  $S_m$ , we utilize positional encoding and MLP layers to generate positional query  $P_m$  as:

$$P_m = \text{MLP}(\text{PE}(S_m)) = \text{MLP}(\text{PE}(c_m) \parallel \text{PE}(w_m)),$$

where  $\text{PE}$  means fixed positional encoding to generate sinusoidal embeddings from the learnable span. Two key modules in our decoder are self-attention and cross-attention. In the self-attention module, the queries and keys additionally take  $P_m$  as:

$$Q_m = D_m + P_m, \quad K_m = D_m + P_m, \quad V_m = D_m,$$

where  $D_m$  is the decoder embedding, an input of the decoder layer. Each component in the cross-attention module can be represented as:

$$Q_m = (D_m \parallel \text{PE}(S_m) \otimes \sigma(\text{MLP}(D_m))), \quad K_m = (X'_+ \parallel \text{PE}(X'_+)), \quad V_m = X'_+.$$

The learnable spans are updated layer-by-layer, and we provide the reference spans  $S_{m,\text{ref}}$  to utilize modulated attention which helps to extract multimodal features with various lengths.

$$S_{m,\text{ref}} = \sigma(\text{MLP}(D_m))$$

Please refer to Liu et al. [36] for the implementation details.

### 3.4 Temporal shifting

Recent studies [37–40] explored techniques for augmenting temporal moments in videos and demonstrated that these techniques work well for localization tasks. Inspired by this, we leverage a temporal shifting method that moves the ground-truth moment to a new (random) temporal position. We apply the temporal shifting method to a video  $V$  in every training step and utilize it as a training sample. We can encourage time-equivariant predictions by allowing the model to predict new temporal locations. Note that we can jointly utilize a temporal shifting method with negative queries since the sequence of frames corresponding to negative queries does not need to be preserved.

### 3.5 Learning objectives

Based on decoder outputs, we apply MLP layers to generate a set of  $M$  predictions denoted as  $\hat{y} = \{\hat{y}_i\}_{i=1}^M$ . Each prediction  $\hat{y}_i$  contains two components: 1) the class label  $\hat{c}_i$  to indicate whether the predicted moment is the ground-truth moment or not, and 2) temporal moment location  $\hat{m}_i = (\hat{t}_s^i, \hat{t}_e^i)$ . Following previous works [6, 26], we find the optimal assignment  $i$  between the ground-truth  $y$  and the predictions  $\hat{y}_i$ , using the matching cost  $\mathcal{C}_{\text{match}}$  as:

$$\mathcal{C}_{\text{match}}(y, \hat{y}_i) = -p(\hat{c}_i) + \mathcal{L}_{\text{moment}}(m, \hat{m}_i).$$

We use Hungarian algorithm to find the optimal pair and calculate the loss between the ground-truth moment and predictions.

$$i = \arg \min_{i \in N} \mathcal{C}_{\text{match}}(y, \hat{y}_i).$$

Details of loss formulation are described below.

Charades-CD				Charades-CG				Charades-STA Unseen		
Training	Val	Test iid	Test ood	Training	Test trivial	Novel composition	Novel word	Training	Seen testing	Unseen testing
4,564 (11,071)	333 (859)	333 (823)	1,442 (3,375)	3,555 (8,281)	1,689 (3,096)	2,480 (3,442)	588 (703)	3,366 (5,525)	486 (867)	1,271 (1,665)

Table 1: The number of videos and query-moment pairs in re-organized datasets and splits. Numbers in brackets denote the number of queries within videos.

**Moment localization loss.** The moment localization loss contains two losses: 1) L1 loss and 2) a generalized IoU loss [41]. This loss is designed to calculate the accuracy of a prediction by comparing it to the ground-truth moment.

$$\mathcal{L}_{\text{moment}}(m, \hat{m}_i) = \lambda_{\text{L1}} \|m - \hat{m}_i\| + \lambda_{\text{iou}} \mathcal{L}_{\text{iou}}(m, \hat{m}_i),$$

where  $\lambda_{\text{L1}}$  and  $\lambda_{\text{iou}}$  are the coefficients to adjust weights.

**Frame margin loss.** The margin loss encourages frames within the ground-truth moment to have high scores via hinge loss. Let  $\mathbf{f}_{\text{fore}}$  and  $\mathbf{f}_{\text{back}}$  are frame features in  $\mathbf{v}'_+$ . We use a linear layer to predict the scores of these frame features. Note that  $\mathbf{f}_{\text{fore}}$  is located within the ground-truth moment, and  $\mathbf{f}_{\text{back}}$  is not. The loss can be formulated as follows:

$$\mathcal{L}_{\text{margin}} = \max(0, \Delta + \mathbf{f}_{\text{back}} \mathbf{W} - \mathbf{f}_{\text{fore}} \mathbf{W}),$$

where  $\mathbf{W} \in \mathbb{R}^{d \times 1}$  and  $\Delta$  is the margin.

**Frame attention loss.** The frame attention loss is to encourage high scores on frames within the ground-truth moment. We calculate the loss from weighted frame attention scores  $\mathbf{o}$ , and the loss is expressed as:

$$\mathcal{L}_{\text{att}} = - \frac{\sum_{i=1}^{L_v} \mathbb{1}_{\{t_s \leq i \leq t_e\}} \log(\mathbf{o}_i)}{\sum_{i=1}^{L_v} \mathbb{1}_{\{t_s \leq i \leq t_e\}}},$$

where  $\mathbb{1}(\cdot)$  is set to 1 if the  $i$ -th frame is located within the ground-truth moment  $m$  and 0 otherwise.

**Overall loss.** The overall loss  $\mathcal{L}$  is determined by linearly combining the individual losses mentioned above, and we optimize our model as:

$$\mathcal{L} = \lambda_{\text{cls}} \mathcal{L}_{\text{cls}} + \lambda_{\text{moment}} \mathcal{L}_{\text{moment}} + \lambda_{\text{att}} \mathcal{L}_{\text{att}} + \lambda_{\text{margin}} \mathcal{L}_{\text{margin}},$$

where  $\lambda_{\text{cls}}$ ,  $\lambda_{\text{att}}$ , and  $\lambda_{\text{margin}}$  are hyper-parameters and  $\lambda_{\text{moment}}$  involves two hyper-parameters  $\lambda_{\text{L1}}$  and  $\lambda_{\text{iou}}$ , and  $\mathcal{L}_{\text{cls}}$  is the cross-entropy function computed by  $\hat{c}_i$  that classifies whether the predicted moment is the ground-truth moment.

## 4 Experimental setup

### 4.1 Datasets

We evaluate our model on two widely used datasets: QVHighlights and Charades-STA, and three re-organized datasets: Charades-STA Unseen, Charades-CD, and Charades-CG. To evaluate the model’s generalization ability, each re-organized dataset contains out-of-distribution cases where existing models struggle to perform robustly. We provide the statistics of re-organized datasets in Table 1, and details of each dataset are described below.

**Charades-STA.** Charades-STA [1] is built upon Charades dataset [42] covering daily indoor activities to evaluate VMR. There are 5,338/1,334 videos with an average length of 30 seconds and 12,408/3,720 video-query pairs included for training and testing, respectively.

**Charades-STA Unseen.** Paul et al. [9] investigated whether models can perform well on unseen videos that were not encountered before. "Unseen videos" is a term used for videos that contain queries consisting of nouns or verbs that were not included in the training set (*i.e.*, unseen queries).

Table 2: Performance results on Charades-STA.

Method	Test		
	IoU@0.5	IoU@0.7	mIoU
2D-TAN [14]	39.70	23.31	-
VSLNet [20]	47.31	30.19	45.51
IVG-DCL [23]	50.24	32.88	-
Moment-DETR [6]	53.63	31.37	-
MMN [15]	50.48	29.65	-
LVTR [25]	49.11	26.59	<u>47.13</u>
TLRR [9]	37.63	21.48	-
Shuffling [39]	56.50	<b>38.80</b>	-
VDI [44]	52.30	31.37	-
BM-DETR (ours)	<b>59.08</b>	<u>37.50</u>	<b>50.91</b>

Table 3: Performance results on Charades-STA Unseen. The performance of Shuffling\* is based on our reproduced results.

Method	Unseen testing		
	IoU@0.5	IoU@0.7	mIoU
DeViSE [45]	29.98	11.29	-
ESZSL [46]	23.90	10.13	-
SCDM [47]	28.22	11.89	28.63
LGI [21]	29.01	12.85	29.62
2D-TAN [14]	31.05	13.33	29.88
Shuffling*[39]	31.53	<u>17.30</u>	<u>35.44</u>
TLRR [9]	<u>33.15</u>	16.22	31.29
BM-DETR (ours)	<b>41.21</b>	<b>23.84</b>	<b>39.12</b>

Also, corresponding moments are excluded from the training set. To comprehend unseen videos, the model should learn transferable knowledge from seen videos.

**Charades-CD.** Yuan et al. [7] found that existing models predict based on frequent patterns in the temporal moment distribution within datasets, known as temporal bias, rather than real comprehension. For a reliable evaluation, they reconstructed a dataset with four splits, including a challenging test split that has different ground-truth moment distribution compared to the training split (*i.e.*, test-ood). The main challenge for models is to perform well on samples from the test-ood split.

**Charades-CG.** Li et al. [8] questioned whether the model can generalize queries formed by including new words or new combinations of words (*i.e.*, compositional generalization). To this end, they constructed new splits, including novel-composition and novel-word test splits containing queries with new composition types (*e.g.*, verb-noun) or new words, respectively. The authors ensured no overlap between the training and testing splits.

**QVHighlights.** QVHighlights is proposed by [6] to evaluate moment retrieval and highlight detection. There are over 10,000 videos with a duration of 150 seconds consisting of lifestyle vlog and news videos and 7,218/1,550/1,542 queries are annotated in train, validation, and test splits, respectively.

## 4.2 Implementation Details

Our model is built upon Moment-DETR [6] implemented in Pytorch and trained using a single Titan Xp. We use video features from SlowFast[43] and CLIP [34] encoder, and text features from CLIP [34]. We report the average performance of 3 runs with different random seeds. Please refer to the supplementary material for detailed experiment settings and model configurations.

**Evaluation Metric.** To compare our model’s performance with previous works, we use three metrics; 1)  $R@n$ ,  $IoU=m$ , which measures the percentage of the top- $n$  predicted moments that have an IoU with the ground-truth moment larger than a given threshold  $m$  (*e.g.*, 0.5), 2) Mean Average IoU (mIoU), and 3) Mean Average Precision (mAP) over IoU thresholds.

## 5 Results

### 5.1 Comparison with the State-of-the-Art Methods

In this section, we compare the BM-DETR to previous models on various datasets. We use bolds to mark the best score in each table, while the second-best score is underlined.

**Charades-STA.** We report the performance on Charades-STA in Table 2, and our model achieves competitive performance compared to previous models. Especially, BM-DETR outperforms previous transformer architecture-based models [6, 25], demonstrating the effectiveness of our model design.

**Charades-STA Unseen.** In Table 3, we report the performance of previous models on Charades-STA Unseen and show the superior transferable knowledge of BM-DETR. Particularly, our model significantly surpasses the previous SoTA method by 25.02% on mIoU.

Table 4: Performance results on Charades-CD. Since the authors [39] did not name the proposed framework, we call it “Shuffling” from the paper’s title.

Method	Test-iid				Test-ood			
	IoU@0.3	IoU@0.5	IoU@0.7	mIoU	IoU@0.3	IoU@0.5	IoU@0.7	mIoU
2D-TAN [14]	60.15	49.09	26.85	42.73	52.79	35.88	13.91	34.22
LG [21]	64.52	51.28	28.68	45.16	59.43	42.90	19.29	39.43
DRN [22]	53.22	42.04	23.32	28.21	45.87	31.11	15.17	23.05
VSLNet [20]	61.48	43.26	28.43	42.92	54.61	34.10	17.87	36.34
DCM [48]	67.27	55.81	37.30	48.74	60.89	45.47	22.70	40.99
Shuffling [39]	<u>70.72</u>	<u>57.59</u>	<b>37.79</b>	<b>50.93</b>	<u>64.59</u>	<u>46.67</u>	<u>27.08</u>	<u>44.30</u>
BM-DETR (ours)	<b>71.87</b>	<b>58.32</b>	<u>35.87</u>	<u>49.42</u>	<b>66.73</b>	<b>49.32</b>	<b>27.12</b>	<b>45.18</b>

Table 5: Performance results on Charades-CG. “-” in each cell means that the result on the metric is not reported in the original paper.

Method	Test-trivial			Novel-composition			Novel-word		
	IoU@0.5	IoU@0.7	mIoU	IoU@0.5	IoU@0.7	mIoU	IoU@0.5	IoU@0.7	mIoU
WSSL [49]	15.33	5.46	18.31	3.61	1.21	8.26	2.79	0.73	7.92
TMN [50]	18.75	8.16	19.82	8.68	4.07	10.14	9.43	4.96	11.23
TSP-PRL [51]	39.86	21.07	38.41	16.30	2.04	13.52	14.83	2.61	14.03
2D-TAN [14]	48.58	26.49	44.27	30.91	12.23	29.75	29.36	13.21	28.47
LGI [21]	49.45	23.80	45.01	29.42	12.73	30.09	26.48	12.47	27.62
VSLNet [20]	45.91	19.80	41.63	24.25	11.54	31.43	25.60	10.07	30.21
VISA [8]	<u>53.20</u>	<u>26.52</u>	<u>47.11</u>	<u>45.41</u>	<u>22.71</u>	<b>42.03</b>	42.35	20.88	40.18
MMN [15]	-	-	-	-	-	-	43.85	24.17	39.50
VDI [44]	-	-	-	-	-	-	<u>46.47</u>	<u>28.63</u>	<u>41.60</u>
BM-DETR (ours)	<b>57.11</b>	<b>36.21</b>	<b>50.33</b>	<b>45.49</b>	<b>22.83</b>	<u>40.28</u>	<b>53.87</b>	<b>31.13</b>	<b>44.12</b>

Table 6: Performance results on test split of QVHighlights. We gray out methods that use additional input sources (*i.e.*, audio) for a fair comparison.

Method	R1		mAP		
	@0.5	@0.7	@0.5	@0.75	avg
MCN [11]	11.41	2.72	24.94	8.22	10.67
CAL [52]	25.49	11.54	23.40	7.65	9.89
XML [53]	41.83	30.35	44.63	31.73	32.14
XML+ [6]	46.69	33.46	47.89	<b>34.67</b>	<b>34.90</b>
Moment-DETR [6]	52.89	33.02	54.82	29.40	30.73
UMT [54]	56.23	41.18	53.83	37.01	36.12
BM-DETR (ours)	<b>57.26</b>	<b>38.85</b>	<b>58.15</b>	<u>33.58</u>	<u>34.75</u>

**Charades-CD.** In Table 4, we summarized the performance of several models on Charades-CD, including models designed to solve the temporal bias problem [39, 48]. BM-DETR shows competitive performances compared to baseline models, and our results also suggest that utilizing temporally augmented videos can enhance the model’s capability for generalization against temporal distributions.

**Charades-CG.** Table 5 reports the performance for existing models in Charades-CG. We show that BM-DETR outperforms previous models, demonstrating superior compositional generalizability. Previous SoTA model [8] utilizes pre-trained models to extract the objects and actions in videos which are required during training, whereas BM-DETR does not.

**QVHighlights.** In Table 6, we show that BM-DETR achieves competitive performance on QVHighlights compared to baseline models. Also, it demonstrates that our model performs well on videos with different characteristics (*e.g.*, news). Yet our model shows slightly lower performance than baseline models on some metrics, and we will discuss this in the limitation section.

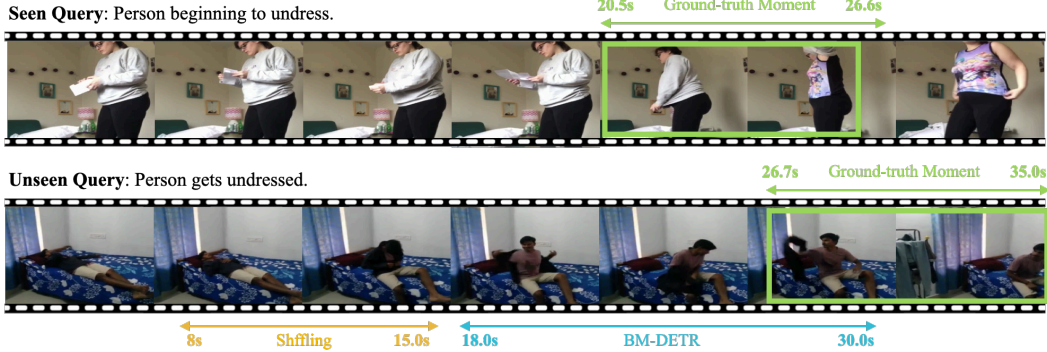


Table 7: Ablations on model components.

NQ	TS	LS	STA	CD	CG	Unseen
✓			53.43	43.67	39.76	36.81
✓	✓		53.67	45.38	39.81	39.53
✓		✓	57.64	45.52	40.30	38.86
✓	✓	✓	<b>59.08</b>	<b>49.32</b>	<b>45.49</b>	<b>41.21</b>

Table 8: Ablations on losses.

$\mathcal{L}'$	$\mathcal{L}_{att}$	$\mathcal{L}_{margin}$	STA	CD	CG	Unseen
✓			27.62	15.44	21.37	24.86
✓	✓		55.87	45.72	41.86	39.18
✓		✓	57.63	45.57	43.41	40.66
✓	✓	✓	<b>59.08</b>	<b>49.32</b>	<b>45.49</b>	<b>41.21</b>

Figure 3: **Top:** Samples in Charades-STA Unseen training split. **Bottom:** Visualization of prediction results.

## 5.2 Ablation Study

In Table 7, 8, and 9, we report the performance (R@1, IoU=0.5) of our model on various splits, including test in Charades-STA, test-ood in Charades-CD, novel-composition in Charades-CG, and unseen testing in Charades-STA Unseen.

**Ablations on model components.** To validate the effectiveness of each model component, we build up several baseline models with different model components. Using negative queries, temporal shifting, and learnable spans are represented by NQ, TS, and LS, respectively. In Table 7, we confirm that all components contribute to performance improvements.

**Ablations on losses.** To investigate the impact of each loss on the model’s performance, we turn off one loss at a time, and the results are reported in Table 8.  $\mathcal{L}'$  means utilizing both  $\mathcal{L}_{cls}$  and  $\mathcal{L}_{moment}$ . We conclude that frame-wise attention loss and frame margin loss play crucial roles in achieving successful VMR, and jointly leveraging them provides further performance improvements.

**Ablations on sampling strategy.** Considering the cases where negative queries are unavailable, we use random queries in the training set and report the model’s performance in Table 9. There is no noticeable performance change.

Rand	STA	CD	CG	Unseen
✓	58.18	48.67	42.82	<b>42.14</b>
	<b>59.08</b>	<b>49.32</b>	<b>45.49</b>	41.21

Table 9: Ablations on sampling strategy.

## 5.3 Visualization Results

In figure 3, we conduct experiments on Charades-STA Unseen dataset to show how BM-DETR behaves given unseen videos. Our model has not encountered the verb “get” before, but the given unseen query conveys the same meaning as in the seen query. We show that BM-DETR’s prediction is more accurate not only than the prediction of baseline (*i.e.*, Shuffling), but also than the ground-truth moment, demonstrating the successful mitigation of weak alignment.

## 6 Conclusion

In this paper, we argue the weak visual-textual alignment problem and present BM-DETR to alleviate it. With the proposed background-aware moment detection, BM-DETR can effectively learn to identify and focus on the most relevant visual features of the target moment. Through extensive experiments results, BM-DETR has demonstrated its strength by showing superior performance. Notably, BM-DETR shows remarkable generalization capabilities and consistently performs well in challenging VMR scenarios.

**Limitations.** Although BM-DETR has achieved promising results in various settings, the effectiveness of our model may not manifest since negative queries are not always available in practical applications. As we can see in Table 6, the performance of BM-DETR is slightly lower than the baseline model on some metrics. One potential reason is that only 2% of the annotations in the train split (148/7,218) can be used as negative queries. In future research, we will address this limitation and explore the extension of our methods to other video-understanding tasks and videos with diverse domains.

## **Acknowledgement**

This work was supported by the SNU-NAVER Hyperscale AI Center and the Institute of Information & Communications Technology Planning & Evaluation (2015-0-00310-SW.StarLab/10%, 2019-0-01371-BabyMind/10%, 2021-0-02068-AIHub/10%, 2021-0-01343-GSAI/20%, 2022-0-00951-LBA/30%, 2022-0-00953-PICA/20%) grant funded by the Korean government.

## References

- [1] Jiyang Gao, Chen Sun, Zhenheng Yang, and Ram Nevatia. Tall: Temporal activity localization via language query. In *Proceedings of the IEEE international conference on computer vision*, pages 5267–5275, 2017.
- [2] Serena Yeung, Olga Russakovsky, Greg Mori, and Li Fei-Fei. End-to-end learning of action detection from frame glimpses in videos. In *Proceedings of the IEEE conference on computer vision and pattern recognition*, pages 2678–2687, 2016.
- [3] Zheng Shou, Dongang Wang, and Shih-Fu Chang. Temporal action localization in untrimmed videos via multi-stage cnns. In *Proceedings of the IEEE conference on computer vision and pattern recognition*, pages 1049–1058, 2016.
- [4] Jun Xu, Tao Mei, Ting Yao, and Yong Rui. Msr-vtt: A large video description dataset for bridging video and language. In *Proceedings of the IEEE conference on computer vision and pattern recognition*, pages 5288–5296, 2016.
- [5] Ranjay Krishna, Kenji Hata, Frederic Ren, Li Fei-Fei, and Juan Carlos Niebles. Dense-captioning events in videos. In *Proceedings of the IEEE international conference on computer vision*, pages 706–715, 2017.
- [6] Jie Lei, Tamara L Berg, and Mohit Bansal. Detecting moments and highlights in videos via natural language queries. *Advances in Neural Information Processing Systems*, 34:11846–11858, 2021.
- [7] Yitian Yuan, Xiaohan Lan, Xin Wang, Long Chen, Zhi Wang, and Wenwu Zhu. A closer look at temporal sentence grounding in videos: Dataset and metric. In *Proceedings of the 2nd International Workshop on Human-centric Multimedia Analysis*, pages 13–21, 2021.
- [8] Juncheng Li, Junlin Xie, Long Qian, Linchao Zhu, Siliang Tang, Fei Wu, Yi Yang, Yueting Zhuang, and Xin Eric Wang. Compositional temporal grounding with structured variational cross-graph correspondence learning, 2022.
- [9] Sudipta Paul, Niluthpol Chowdhury Mithun, and Amit K Roy-Chowdhury. Text-based temporal localization of novel events. In *Computer Vision–ECCV 2022: 17th European Conference, Tel Aviv, Israel, October 23–27, 2022, Proceedings, Part XIV*, pages 567–587. Springer, 2022.
- [10] Huijuan Xu, Kun He, Bryan A Plummer, Leonid Sigal, Stan Sclaroff, and Kate Saenko. Multilevel language and vision integration for text-to-clip retrieval. In *Proceedings of the AAAI Conference on Artificial Intelligence*, volume 33, pages 9062–9069, 2019.
- [11] Lisa Anne Hendricks, Oliver Wang, Eli Shechtman, Josef Sivic, Trevor Darrell, and Bryan Russell. Localizing moments in video with natural language. In *Proceedings of the IEEE international conference on computer vision*, pages 5803–5812, 2017.
- [12] Jingyuan Chen, Xinpeng Chen, Lin Ma, Zequn Jie, and Tat-Seng Chua. Temporally grounding natural sentence in video. In *Proceedings of the 2018 conference on empirical methods in natural language processing*, pages 162–171, 2018.
- [13] Zhu Zhang, Zhijie Lin, Zhou Zhao, and Zhenxin Xiao. Cross-modal interaction networks for query-based moment retrieval in videos. In *Proceedings of the 42nd International ACM SIGIR Conference on Research and Development in Information Retrieval*, pages 655–664, 2019.
- [14] Songyang Zhang, Houwen Peng, Jianlong Fu, and Jiebo Luo. Learning 2d temporal adjacent networks for moment localization with natural language. In *Proceedings of the AAAI Conference on Artificial Intelligence*, volume 34, pages 12870–12877, 2020.
- [15] Zhenzhi Wang, Limin Wang, Tao Wu, Tianhao Li, and Gangshan Wu. Negative sample matters: A renaissance of metric learning for temporal grounding. In *Proceedings of the AAAI Conference on Artificial Intelligence*, volume 36, pages 2613–2623, 2022.
- [16] Yitian Yuan, Tao Mei, and Wenwu Zhu. To find where you talk: Temporal sentence localization in video with attention based location regression. In *Proceedings of the AAAI Conference on Artificial Intelligence*, volume 33, pages 9159–9166, 2019.

- [17] Dongliang He, Xiang Zhao, Jizhou Huang, Fu Li, Xiao Liu, and Shilei Wen. Read, watch, and move: Reinforcement learning for temporally grounding natural language descriptions in videos. In *Proceedings of the AAAI Conference on Artificial Intelligence*, volume 33, pages 8393–8400, 2019.
- [18] Cristian Rodriguez, Edison Marrese-Taylor, Fatemeh Sadat Saleh, Hongdong Li, and Stephen Gould. Proposal-free temporal moment localization of a natural-language query in video using guided attention. In *Proceedings of the IEEE/CVF winter conference on applications of computer vision*, pages 2464–2473, 2020.
- [19] Long Chen, Chujie Lu, Siliang Tang, Jun Xiao, Dong Zhang, Chile Tan, and Xiaolin Li. Rethinking the bottom-up framework for query-based video localization. In *Proceedings of the AAAI Conference on Artificial Intelligence*, volume 34, pages 10551–10558, 2020.
- [20] Hao Zhang, Aixin Sun, Wei Jing, and Joey Tianyi Zhou. Span-based localizing network for natural language video localization. *arXiv preprint arXiv:2004.13931*, 2020.
- [21] Jonghwan Mun, Minsu Cho, and Bohyung Han. Local-global video-text interactions for temporal grounding. In *Proceedings of the IEEE/CVF Conference on Computer Vision and Pattern Recognition*, pages 10810–10819, 2020.
- [22] Runhao Zeng, Haoming Xu, Wenbing Huang, Peihao Chen, Mingkui Tan, and Chuang Gan. Dense regression network for video grounding. In *Proceedings of the IEEE/CVF Conference on Computer Vision and Pattern Recognition*, pages 10287–10296, 2020.
- [23] Guoshun Nan, Rui Qiao, Yao Xiao, Jun Liu, Sicong Leng, Hao Zhang, and Wei Lu. Interventional video grounding with dual contrastive learning. In *Proceedings of the IEEE/CVF conference on computer vision and pattern recognition*, pages 2765–2775, 2021.
- [24] Fengyuan Shi, Limin Wang, and Weilin Huang. End-to-end dense video grounding via parallel regression. *arXiv preprint arXiv:2109.11265*, 2021.
- [25] Sangmin Woo, Jinyoung Park, Inyong Koo, Sumin Lee, Minki Jeong, and Changick Kim. Explore and match: End-to-end video grounding with transformer. *arXiv preprint arXiv:2201.10168*, 2022.
- [26] Xizhou Zhu, Weijie Su, Lewei Lu, Bin Li, Xiaogang Wang, and Jifeng Dai. Deformable detr: Deformable transformers for end-to-end object detection. *arXiv preprint arXiv:2010.04159*, 2020.
- [27] Antoine Miech, Jean-Baptiste Alayrac, Lucas Smaira, Ivan Laptev, Josef Sivic, and Andrew Zisserman. End-to-end learning of visual representations from uncurated instructional videos. In *Proceedings of the IEEE/CVF Conference on Computer Vision and Pattern Recognition*, pages 9879–9889, 2020.
- [28] Dohwan Ko, Joonmyung Choi, Juyeon Ko, Shinyeong Noh, Kyoung-Woon On, Eun-Sol Kim, and Hyunwoo J Kim. Video-text representation learning via differentiable weak temporal alignment. In *Proceedings of the IEEE/CVF Conference on Computer Vision and Pattern Recognition*, pages 5016–5025, 2022.
- [29] Tengda Han, Weidi Xie, and Andrew Zisserman. Temporal alignment networks for long-term video. In *Proceedings of the IEEE/CVF Conference on Computer Vision and Pattern Recognition*, pages 2906–2916, 2022.
- [30] Xinpeng Ding, Nannan Wang, Shiwei Zhang, De Cheng, Xiaomeng Li, Ziyuan Huang, Mingqian Tang, and Xinbo Gao. Support-set based cross-supervision for video grounding. In *Proceedings of the IEEE/CVF International Conference on Computer Vision*, pages 11573–11582, 2021.
- [31] Humam Alwassel, Silvio Giancola, and Bernard Ghanem. Tsp: Temporally-sensitive pretraining of video encoders for localization tasks. In *Proceedings of the IEEE/CVF International Conference on Computer Vision*, pages 3173–3183, 2021.
- [32] Surya T Tokdar and Robert E Kass. Importance sampling: a review. *Wiley Interdisciplinary Reviews: Computational Statistics*, 2(1):54–60, 2010.

- [33] Aaron van den Oord, Yazhe Li, and Oriol Vinyals. Representation learning with contrastive predictive coding. *arXiv preprint arXiv:1807.03748*, 2018.
- [34] Alec Radford, Jong Wook Kim, Chris Hallacy, Aditya Ramesh, Gabriel Goh, Sandhini Agarwal, Girish Sastry, Amanda Askell, Pamela Mishkin, Jack Clark, et al. Learning transferable visual models from natural language supervision. In *International conference on machine learning*, pages 8748–8763. PMLR, 2021.
- [35] Ashish Vaswani, Noam Shazeer, Niki Parmar, Jakob Uszkoreit, Llion Jones, Aidan N Gomez, Łukasz Kaiser, and Illia Polosukhin. Attention is all you need. *Advances in neural information processing systems*, 30, 2017.
- [36] Shilong Liu, Feng Li, Hao Zhang, Xiao Yang, Xianbiao Qi, Hang Su, Jun Zhu, and Lei Zhang. Dab-detr: Dynamic anchor boxes are better queries for detr. *arXiv preprint arXiv:2201.12329*, 2022.
- [37] Mengmeng Xu, Juan-Manuel Pérez-Rúa, Victor Escorcia, Brais Martinez, Xiatian Zhu, Li Zhang, Bernard Ghanem, and Tao Xiang. Boundary-sensitive pre-training for temporal localization in videos. In *Proceedings of the IEEE/CVF International Conference on Computer Vision*, pages 7220–7230, 2021.
- [38] Hao Zhang, Aixin Sun, Wei Jing, and Joey Tianyi Zhou. Towards debiasing temporal sentence grounding in video. *arXiv preprint arXiv:2111.04321*, 2021.
- [39] Jiachang Hao, Haifeng Sun, Pengfei Ren, Jingyu Wang, Qi Qi, and Jianxin Liao. Can shuffling video benefit temporal bias problem: A novel training framework for temporal grounding. In *Computer Vision–ECCV 2022: 17th European Conference, Tel Aviv, Israel, October 23–27, 2022, Proceedings, Part XXXVI*, pages 130–147. Springer, 2022.
- [40] Can Zhang, Tianyu Yang, Junwu Weng, Meng Cao, Jue Wang, and Yuexian Zou. Unsupervised pre-training for temporal action localization tasks. In *Proceedings of the IEEE/CVF Conference on Computer Vision and Pattern Recognition*, pages 14031–14041, 2022.
- [41] Hamid Rezatofighi, Nathan Tsoi, JunYoung Gwak, Amir Sadeghian, Ian Reid, and Silvio Savarese. Generalized intersection over union: A metric and a loss for bounding box regression. In *Proceedings of the IEEE/CVF conference on computer vision and pattern recognition*, pages 658–666, 2019.
- [42] Gunnar A Sigurdsson, Gül Varol, Xiaolong Wang, Ali Farhadi, Ivan Laptev, and Abhinav Gupta. Hollywood in homes: Crowdsourcing data collection for activity understanding. In *Computer Vision–ECCV 2016: 14th European Conference, Amsterdam, The Netherlands, October 11–14, 2016, Proceedings, Part I 14*, pages 510–526. Springer, 2016.
- [43] Christoph Feichtenhofer, Haoqi Fan, Jitendra Malik, and Kaiming He. Slowfast networks for video recognition. In *Proceedings of the IEEE/CVF international conference on computer vision*, pages 6202–6211, 2019.
- [44] Dezhao Luo, Jiabo Huang, Shaogang Gong, Hailin Jin, and Yang Liu. Towards generalisable video moment retrieval: Visual-dynamic injection to image-text pre-training. *arXiv preprint arXiv:2303.00040*, 2023.
- [45] Andrea Frome, Greg S Corrado, Jon Shlens, Samy Bengio, Jeff Dean, Marc’Aurelio Ranzato, and Tomas Mikolov. Devise: A deep visual-semantic embedding model. *Advances in neural information processing systems*, 26, 2013.
- [46] Bernardino Romera-Paredes and Philip Torr. An embarrassingly simple approach to zero-shot learning. In *International conference on machine learning*, pages 2152–2161. PMLR, 2015.
- [47] Yitian Yuan, Lin Ma, Jingwen Wang, Wei Liu, and Wenwu Zhu. Semantic conditioned dynamic modulation for temporal sentence grounding in videos. *Advances in Neural Information Processing Systems*, 32, 2019.

- [48] Xun Yang, Fuli Feng, Wei Ji, Meng Wang, and Tat-Seng Chua. Deconfounded video moment retrieval with causal intervention. In *Proceedings of the 44th International ACM SIGIR Conference on Research and Development in Information Retrieval*, pages 1–10, 2021.
- [49] Xuguang Duan, Wenbing Huang, Chuang Gan, Jingdong Wang, Wenwu Zhu, and Junzhou Huang. Weakly supervised dense event captioning in videos. *Advances in Neural Information Processing Systems*, 31, 2018.
- [50] Bingbin Liu, Serena Yeung, Edward Chou, De-An Huang, Li Fei-Fei, and Juan Carlos Niebles. Temporal modular networks for retrieving complex compositional activities in videos. In *Proceedings of the European Conference on Computer Vision (ECCV)*, pages 552–568, 2018.
- [51] Jie Wu, Guanbin Li, Si Liu, and Liang Lin. Tree-structured policy based progressive reinforcement learning for temporally language grounding in video. In *Proceedings of the AAAI Conference on Artificial Intelligence*, volume 34, pages 12386–12393, 2020.
- [52] Victor Escorcia, Mattia Soldan, Josef Sivic, Bernard Ghanem, and Bryan Russell. Temporal localization of moments in video collections with natural language. *arXiv preprint arXiv:1907.12763*, 2019.
- [53] Jie Lei, Licheng Yu, Tamara L Berg, and Mohit Bansal. Tvr: A large-scale dataset for video-subtitle moment retrieval. In *ECCV*, 2020.
- [54] Ye Liu, Siyuan Li, Yang Wu, Chang-Wen Chen, Ying Shan, and Xiaohu Qie. Umt: Unified multi-modal transformers for joint video moment retrieval and highlight detection. In *Proceedings of the IEEE/CVF Conference on Computer Vision and Pattern Recognition*, pages 3042–3051, 2022.

## APPENDIX

In this Appendix, we describe the following sections:

1. Additional information about our experimental setup (Section A)
2. Additional experimental results (Section B)
3. Examples of BM-DETR’s prediction (Section C)

### A Experimental setup

We use video features from SlowFast[43] and CLIP [34] encoder, and text features from CLIP [34]. The encoder and decoder in our model are stacked with 3 layers of transformer block. We utilize AdamW to optimize our model. We set the hidden dimension of transformers as 256, and the model weights are initialized with Xavier init. We use a fixed number of 10 learnable spans, the same number of predicted moments. Loss hyper-parameters are  $\lambda_{L1} = 1$ ,  $\lambda_{iou} = 8$ ,  $\lambda_{cls} = 8$ ,  $\lambda_{att} = 1$ , and  $\lambda_{margin} = 4$  and the margin  $\Delta$  is 0.2.

**QVHighlights.** For QVHighlights, we extract visual features at 2 FPS. We train the model with batch size 32 for 200 epochs with a learning rate as  $2e-4$  and weight decay as  $1e-4$ . In addition, some queries in QVHighlights are matched to multiple ground-truth moments. Let  $N$  be the total number of ground-truth moments, which is less than 5. In this case, our model finds the optimal bipartite matching between ground-truth moments and predictions. Then we calculate the losses based on optimal assignment.

**Charades-STA.** For Charades-STA and re-organized datasets, including Charades-CD, Charades-CG, and Charades-STA Unseen, we extract visual features at 1 FPS. We select the best-performing model on Charades-STA to conduct evaluations on re-organized datasets. We set the batch size 32 with a learning rate as  $2e-4$  and weight decay as  $1e-4$ . The model is trained for 100 epochs on Charades-STA and for less than 50 epochs on the other datasets.

Enc	Dec	Charades-STA		
		IoU@0.5	IoU@0.7	mIoU
1	1	51.73	29.44	46.05
2	2	56.32	35.92	49.27
3	3	<b>59.08</b>	<b>37.50</b>	<b>50.91</b>
4	4	57.89	37.26	50.17
5	5	58.14	36.65	50.29
6	6	56.47	35.11	49.16

Table 10: Ablation study on the effect of Encoder-Decoder layers.

Num of Embeddings	Charades-STA		
	IoU@0.5	IoU@0.7	mIoU
5	57.35	36.75	49.83
10	<b>59.08</b>	<b>37.50</b>	<b>50.91</b>
15	58.52	37.32	50.35
20	56.92	35.49	49.40
25	57.26	36.42	49.60
30	57.98	36.58	50.29

Table 11: Ablation study on the effect of the number of learnable spans.

$\lambda_{L1}$	$\lambda_{iou}$	$\lambda_{cls}$	$\lambda_{att}$	$\lambda_{margin}$	Test		
					IoU @0.5	IoU@0.7	mIoU
1	8	8	1	4	<b>59.08</b>	<b>37.50</b>	<b>50.91</b>
2	8	8	1	4	56.93	35.95	49.54
4	4	4	1	4	57.55	36.64	49.59
4	16	16	1	4	57.15	36.42	49.54
8	8	16	1	4	57.95	36.89	50.04

Table 12: Ablation study for hyperparameters

## B Experiments

We provide additional experiment results in the following sections, which are not in the main paper:

**Ablations on model size.** In Table 10, we conduct experiments to find the proper number of layers for each encoder and decoder. We observed a tendency that performance is improved monotonically as the number of layers increases. Once the number of layers surpasses a specific threshold, no more significant performance improvement exists.

**Ablations on learnable spans.** We summarize the performance of models trained with varying numbers of learnable spans in Table 11. We found that utilizing 10 learnable spans shows the best performance. Also, we observed using more learnable spans didn’t improve the performance.

**Ablations on hyperparameters.** We ran hyperparameter tuning for all possible combinations of  $\lambda_{L1}$ ,  $\lambda_{cls}$ , and  $\lambda_{iou}$  with values of 1, 2, 4, 8, and 16. For  $\lambda_{att}$  and  $\lambda_{margin}$ , we fixed the default values of 1 and 4. For each combination, the experiments were averaged three times and the five best-performing cases are reported in Table 12.

## C Additional visualization results

In Figure 4, we provide four additional visualization results of our model’s prediction on Charades-STA and QVHighlights.

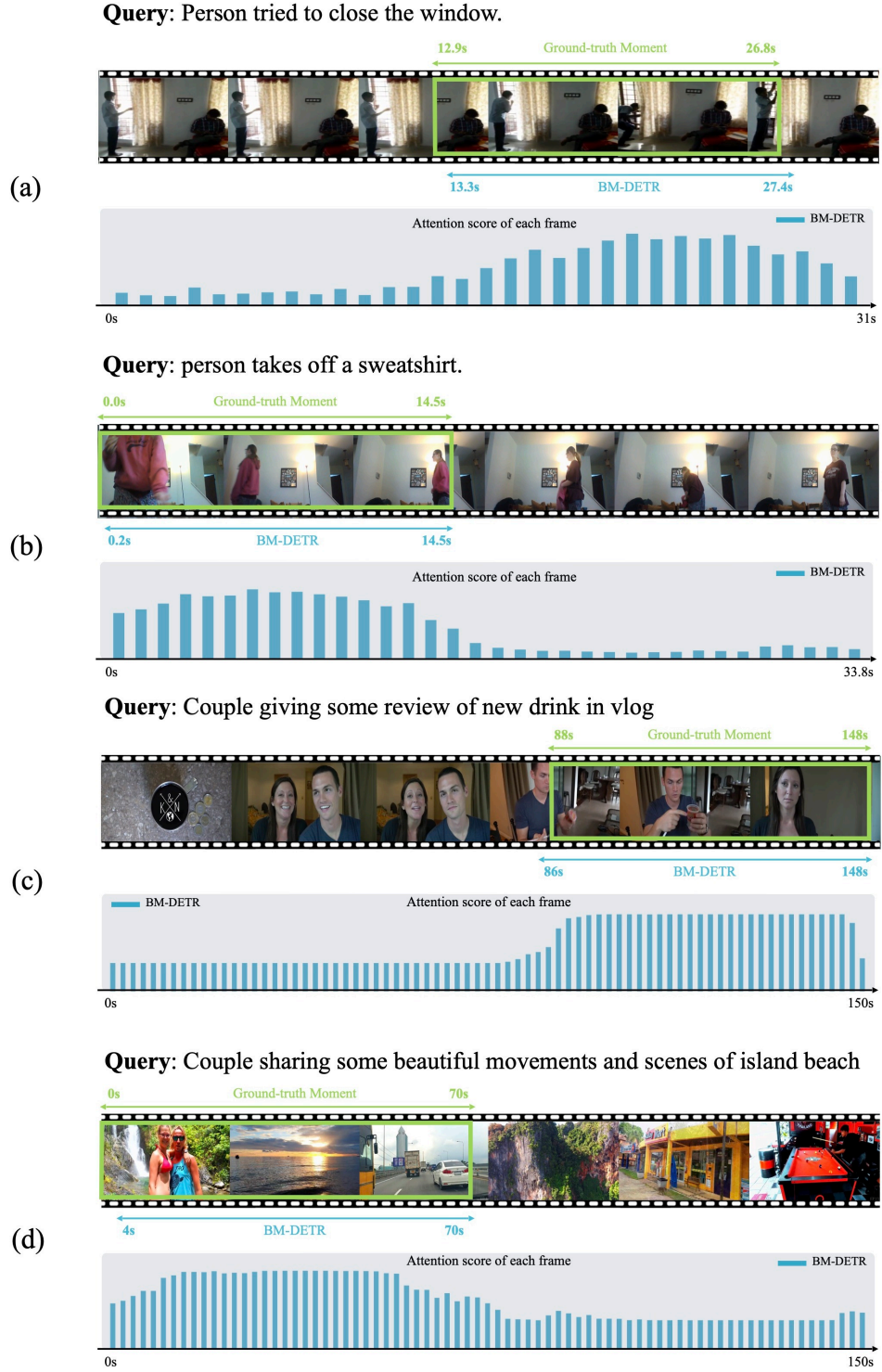


Figure 4: Four visualization examples of our model’s moment prediction. We show predicted temporal moment and ground-truth moment. Also, we present frame attention scores below.